Chapter 2
Greenhouse Gases and Climatic Change

Vincent Moron

Abstract Earth climate is determined by the equilibrium between the amount and distribution of incoming radiation absorbed from the sun and the outgoing longwave radiation emitted at the top of the atmosphere. Several atmospheric trace gases, including water vapor, carbon dioxide, methane, and nitrous oxide, absorb far more efficiently the longwave radiation than solar radiation. These so-called greenhouse gases increase the amount of energy available to the earth and keep it much warmer than it would be otherwise. Although water vapor (and clouds that contribute both to the greenhouse effect and cooling through the back reflection of the incoming solar radiation) does not stay in the atmosphere more than ~2 weeks, most of the other greenhouse gases stay far more than 10 years. Anthropogenic use of fossil fuels, cement production, and deforestation already increased the atmospheric concentration of greenhouse gases and human activities also created new synthetic and powerful ones such as chlorofluorocarbon. The corresponding positive radiative already contributed to the ~0.8 °C increase of the global surface temperature since 1850 and will act as the main climate driver for at least the next century. This chapter outlines the bases of the greenhouse effect and its impact on the earth climate from ~1850 to 2100.

Keywords Greenhouse gas • Earth climate • Radiative balance • Climate model • Kyoto protocol

V. Moron
Département de Géographie, Pôle SGAE, UFR ALLSH,
Aix-Marseille University, Aix en Provence, France

CEREGE, UMR 7330 CNRS, Aix en Provence, France

Institut Universitaire de France, Paris, France

International Research Institute for Climate and Society,
Columbia University, Palisades, NY, USA
email: moron@cerege.fr

J.B. Saulnier and M.D. Varella (eds.), *Global Change, Energy Issues and Regulation Policies*, Integrated Science & Technology Program 2, DOI 10.1007/978-94-007-6661-7_2,
© Springer Science+Business Media Dordrecht 2013

List of Acronyms

AOGCM	Atmosphere–Ocean General Circulation Model
CDIAC	Carbon Dioxide Information Analysis Center
CEREGE	Centre Européen de Recherche et d'Enseignement des Géosciences de l'Environnement
CFC	Chlorofluorocarbon
CO_2	Carbon dioxide molecule
CH_4	Methane molecule
CRU	Climatic Research Unit
ESRL	Earth System Research Laboratory
GCM	Global Climate Model
GISS	Goddard Institute for Space Studies
GHG	Greenhouse gas
Gt	Gigaton (1 Gt = 10^9 t)
GtC	Gigaton of equivalent carbon
HCFC	Hydro-carbo-fluoro-carbone molecule
HFC	Hydro-fluoro-carbone molecule
H_2O	Water molecule
IPCC	Intergovernmental panel on climate change
IR	Infrared radiation
m a.s.l	Meter above sea level
N_2O	Nitrous oxide molecule
O_3	Ozone molecule
ppm	Parts per million (in volume)
ppt	Parts per trillion (in volume)
SRES	Special Report on Emissions Scenarios
UNEP	United Nations Environment Programme

2.1 Introduction

In 1975, W.S. Broecker wrote, "*If man-made dust is unimportant as a major cause of climatic change, then a strong case can be made that the present cooling trend will, within a decade or so, give way to a pronounced warming induced by carbon dioxide. By analogy with similar events in the past, the natural climatic cooling which, since 1940, has more than compensated for the carbon dioxide effect, will soon bottom out. Once this happens, the exponential rise in the atmospheric carbon dioxide content will tend to become a significant factor and by early in the next century will have driven the mean planetary temperature beyond the limits experienced during the last 1,000 years.*" This visionary prediction follows some earlier calculations (Fourier 1827; Arrhenius 1896) establishing the physical relationship between certain atmospheric traces (i.e., the greenhouse gases, GHG hereafter) and the earth temperature

variations. There is an increase in GHG atmospheric concentration[1] because human activities (fossil fuel burning, land clearing, deforestation, etc.) release it at a rate[2] surpassing the natural capacity of the earth's system to remove it from the atmosphere. Some of the current knowledge about the earth's radiative balance and GHG atmospheric concentration as well as its link with temperature variations from 1850 to 2100 and the basic mechanisms of the climatic response to current and near-future GHG atmospheric concentrations are reviewed here.

2.2 The Radiative Balance and the Greenhouse Gases

The climate system is a thermodynamical engine fueled by solar radiation (Trenberth et al. 2009). The energy gained from inner earth through volcanism and geothermal sources is considered to be negligible at global scale. At equilibrium, the total absorbed solar radiation at the outer limit of the climate system is counterbalanced by the same amount of emitted radiation.[3] All objects above 0 K emit electromagnetic radiation. Planck's, Stefan–Boltzmann's and Wien's laws define the relationship between the amount and spectrum of emitted radiation and the surface temperature of the emitter.[4] The radiative equilibrium between absorbed solar radiation and outgoing emitted infrared radiation defines a radiative equilibrium temperature, which is approximately 255 K with the assumption that emissivity of the climate system is close to 1.[5] A mean temperature of 255 K is not observed at the earth surface (the mean observed temperature at the earth surface is actually close to 288 K) but rather close to an altitude of 5 km in mean. The fact that observed surface

[1] See, for example, http://www.esrl.noaa.gov/gmd/ccgg/trends/.

[2] Recent estimates show that global fossil and cement emissions equal 9.5 +/− 0.5 GtC/year (that is +54 % from 1990) while global land-use change emissions equal 0.9 +/− 0.5 GtC/year in 2011 (Le Quéré et al. 2012).

[3] This quantity equals the solar "constant" (1,366 W/m^2 = solar energy intercepted by the earth disk) divided by 4, for geometry constraint, multiplied by 1 minus albedo (= 0.3), the albedo being the fraction of radiation reflected by the earth's system, that is, 1366/4 × 0.7~239 W/m^2. The earth's surface absorbs 50 % of total solar radiation and the atmosphere absorbs 20 % of it.

[4] The amount of emitted radiant energy is proportional to the emissivity and fourth power of the surface temperature of the emitter and its spectral peak is inversely proportional to its surface temperature. The emissivity is the ability of a material to emit energy by radiation. This ability is relative to an idealized physical body at the same temperature, called a *black body*, that absorbs all incident electromagnetic radiation and is also the best possible emitter of thermal radiation. The solar surface, roughly near 5,750 K, emits roughly 160,000 times more radiation than the earth surface per unit of surface, mostly in the ultraviolet (spectral power < 0.4 μm), "visible" (i.e., light a human eye could see, within 0.4 and 0.7 μm) and infrared bands (IR, spectral band > 0.7 μm), whereas earth surface and atmosphere (roughly between 180 and 340 K) emit IR only.

[5] The emissivity of land, ocean surface and thicker clouds than cirrus is close to 1, that is, the one of a black body. The clear-sky atmosphere has an emissivity of 0.4–0.8, and cirrus clouds have a typical emissivity of 0.2.

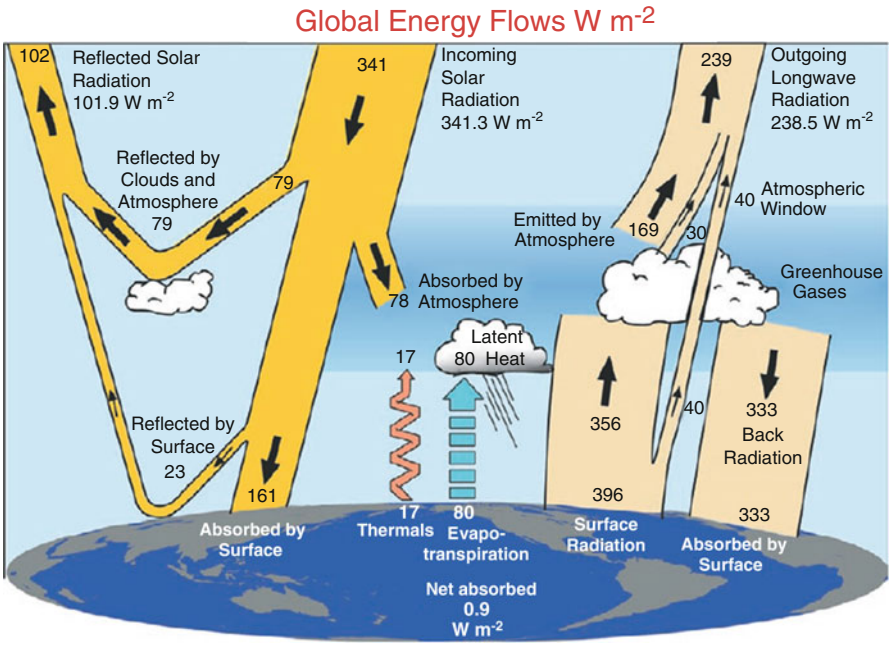

Fig. 2.1 Global annual mean Earth's energy budget (W/m^2) for the period of March 2000 to May 2004 (from Trenberth et al. 2009). The *broad arrows* indicate the schematic flows of energy in proportion to their importance (Reprinted with permission of the American Meteorological Society)

temperature is higher than radiative mean temperature is explained by the greenhouse effect.[6]

Atmosphere is composed of a mixture of various gases. The most abundant gases are di-atomic nitrogen and oxygen accounting for ~98 % in volume of dry air. The GHGs, accounting for less than 1 % of the atmospheric volume, have the property to absorb infrared radiation efficiently, whereas the atmosphere overall absorbs only 20 % of solar radiation (Fig. 2.1). The most important "natural" GHG is water vapor (H_2O), then carbon dioxide (CO_2), methane (CH_4), nitrous oxide (N_2O), and ozone (O_3). Human activities (burning of fossil fuels in industry and agriculture, heat production and transport, deforestation, cement production) add some of these GHGs, but also create synthetic GHGs, as chlorofluorocarbons (CFCs). These "natural" and "synthetic" GHGs (except H_2O and O_3) remain at least 12 years in the atmosphere and thus affect the planetary radiative balance independently on the location of their emission into the atmosphere because the time to mix the whole troposphere is faster than 1 year. Any increase of the energetic content, for example, related to increased GHG atmospheric concentration, leads to a

[6] See http://www.realclimate.org/index.php/archives/2010/07/a-simple-recipe-for-ghe/ for a simple explanation of how the greenhouse effect works. For a more comprehensive review, see, for example, Danny Harvey (2000).

temperature increase until a new equilibrium is eventually reached, so that the climatic system emits IR as much as absorbed net radiation at its outer limit (i.e., the top of the atmosphere for the earth).

It should be noted that although gaseous H_2O is the most efficient[7] GHG, it could not be considered as a major driver of temperature variations because, as liquid and solid water, it is unable to remain in the atmosphere for a long time (typically less than 2 weeks). But increased atmospheric temperature could increase the atmospheric concentration of gaseous H_2O leading to a positive feedback, because warmer air could contain more gaseous H_2O and an higher atmospheric concentration of H_2O increases the greenhouse effect. In other words, despite its largest contribution to the current greenhouse effect, H_2O is more a passive actor of temperature variations whereas other GHGs are active drivers (i.e., they are able to physically drive temperature variations) of temperature variations in current conditions[8] due to their capacity to accumulate in the atmosphere coupled with their physical properties.

2.3 Temporal Variations of the Greenhouse Gases

Many human activities release carbon into the atmosphere. Figure 2.2 displays the monthly mean mole fraction of CO_2 (in parts-per-million—ppm—of volume) measured at three distant stations: Mauna Loa (Hawaii), Barrow (Alaska), and South Pole. These three locations are far away from any large industrial local source of anthropogenic carbon. The long-term positive trend due to global anthropogenic carbon consumption is superimposed to an annual cycle with maximum/minimum recorded at the end of the boreal winter and summer periods at Barrow and Mauna Loa. This annual cycle is due to the vegetation cycle in the northern hemisphere inasmuch as photosynthesis exceeds respiration in spring and summer whereas the opposite, that is, a net CO_2 release by the vegetation, occurs in autumn and winter.

[7] One of the last estimates of the relative contribution of atmospheric long-wave absorbers to the current-day greenhouse effect is: 50 % for water vapor, 25 % for clouds, and 20 % for CO_2. (Schmidt et al. 2010; available at http://pubs.giss.nasa.gov/docs/2010/2010_Schmidt_etal_1.pdf).

[8] At glacial–interglacial scale (i.e., between 10,000 and 100,000 years), CO_2 variations tend to follow temperature variations in Antarctica by ~200–1,000 years at the glacial termination. At this scale, temperature variations are mostly driven by orbital changes (Milankovitch theory). The time lag between CO_2 and temperature seems at least partly due to the adjustment of the ocean deep circulation that releases some CO_2 into the atmosphere when the earth warms. This relationship does not invalidate the current one because the increased concentration of atmospheric CO_2 released by human activities drives the current warming whereas glacial termination was initiated by orbital changes 20,000 years ago. Moreover, it is assumed that GHG variations at glacial–interglacial scale had exerted a positive feedback on temperature variations with other processes as the ice–albedo–temperature feedback, that is, the fact that deglaced areas decrease the mean earth albedo, increasing the amount of absorbed solar radiation (Lorius et al. 1990). Lastly, recent analyses (Shakun et al. 2012) demonstrate that global temperatures mostly lag CO2 variations in Antarctica during the last deglaciation.

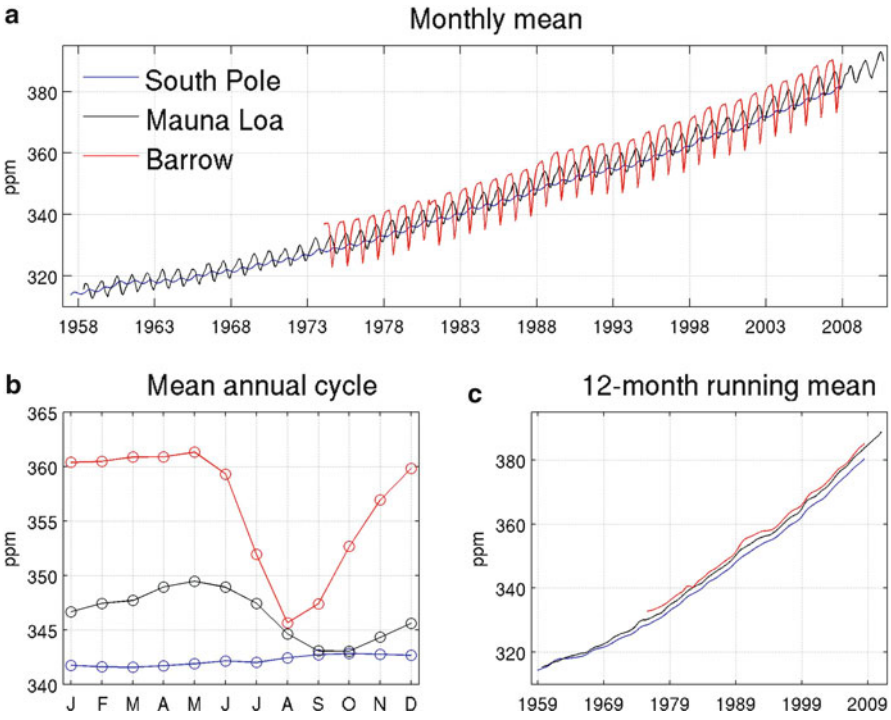

Fig. 2.2 Atmospheric concentration of CO_2 measured at Barrow (Alaska, 71°19′N, 156°36′W, 11 m a.s.l. in *red*), South Pole (89°59′S, 24°48′W, 2810 m a.s.l. in *blue*), and Mauna Loa (19°32′N, 155°35′W, 3397 m a.s.l. in *black*) observatories from September 1957 to July 2010: (**a**) monthly means, (**b**) mean annual cycle, and (**c**) 12-month running mean. The mole fraction of CO_2, expressed as parts per million (ppm), is the number of molecules of CO_2 in every one million molecules of dried air (water vapor removed) (Mauna Loa data come from ESRL, and Barrow and South Pole data are extracted from CDIAC)

The annual cycle is large at Barrow, which is closer to large Eurasiatic and North America continental masses and almost flat at South Pole.

The long-term increase is very consistent among the three records (Fig. 2.2) and not perfectly linear with some steps. On a longer time scale, CO_2 concentration ranges between 270 and 290 ppm in interglacial periods to 190–200 ppm during glacial periods, although concentrations could have been far larger before the quaternary. The atmospheric concentration of other GHG increases due to their use in various human activities already drives the contemporaneous warming of the global surface temperature. Table 2.1 gives the atmospheric concentrations of the most important GHG in October 2008–September 2009 compared to the preindustrial period.

Each GHG has a different lifetime and each molecule has a different radiative forcing. The relative impact of each GHG could also be compared with the integrated radiative forcing from the preindustrial period (IPCC 2007). With that frame, CO_2 is the largest forcing, due to its absolute concentration and its long lifetime

Table 2.1 GHG concentration (in parts-per-million, ppm, and parts-per-trillion, ppt) in 1750 and in 2008/2009 with their lifetime and radiative forcing from preindustrial to current conditions

GHGs	Preindustrial (~1750; ppm)	Current concentrations (2008/2009)	Lifetime (in years)	Radiative forcing (in W/m^2)
CO_2	280	385 ppm	~100	+1.66
CH_4	0.7	1.8 ppm	12	+0.48
N_2O	0.27	0.32 ppm	114	+0.16
Tropospheric O_3	0.025	0.034 ppm	<Few days	+0.35
Synthetic GHG (CFC, HCFC, HFC, SF_6, etc.)	0	Few ppt to 536 ppt	From few years to thousands of years	~+0.30 (most from CFC-11 and CFC-12[a])

Data come from http://cdiac.ornl.gov/pns/current_ghg.html

[a]Some of these synthetic GHGs including CFC-11 and CFC-12 have been banned after the Montreal conference (1987) and its amendments under the UN convention on the stratospheric ozone hole. CFCs are replaced by other components that are not harmful to stratospheric ozone but usually have a huge global warming potential

even if each CO_2 molecule is not the more efficient heat trapper, and synthetic GHGs (CFCs, HCFCs, HFCs, etc.) have a significant impact despite their very small concentrations. The increase of atmospheric GHG increases the energy content of the climate system.[9] The uncertainty on the net anthropogenic forcing is low (IPCC 2007) and as stated before, its extent is global.

2.4 Observed Temperature Variations

Temperature has been recorded for more than 400 years. The longest continuous temperature record is the "Central England Temperature," available since 1659 (Plaut et al. 1995). The temperatures are recorded worldwide in normalized environments so that they can be compared and spatial averages can be computed.[10]

[9]Since 1750 the total radiative forcing related to the increase of atmospheric GHG concentrations due to human activities equals +2.9 W/m^2. The net anthropogenic effect including cooling effect mostly due to sulfur emissions equals +1.6 W/m^2. The direct cooling effect of anthropogenic sulfur associated with the aerosol veil, that increase albedo at a regional scale is complicated by its indirect effect through the modification of the optical properties of clouds. The cooling effect is less certain than the one associated with GHG increase (IPCC 2007).

[10]There is a debate about the sense of a "global" (in the sense of planetary) mean of surface temperature. Everybody could experience very large temperature variations on small time and spatial scales, for example, simply moving from shade to sunlight in a summer day. It seems then unreasonable to compute a spatial mean from a few samples. But, the range of temperature variations strongly decreases when time means (instantaneous record to annual mean) are considered, especially when raw temperatures are scaled to the local mean annual cycle (theoretically estimated with at least 30 years of data). It is because the drivers of temperature variations at this timescale are from regional (e.g., atmospheric Rossby waves, which are giant meanders in the atmosphere.

Sea surface temperature recordings have been generalized since the Brussels maritime workshop in 1853. Several research centers across the world (such as GISS and CRU) have established gridded datasets of surface temperatures freely available on the web. There is considerable work to remove known biases related to urbanization and changes of thermometers. The uncertainty is less than one order of magnitude relatively to long-term increases in these gridded datasets.

Figure 2.3 shows the annual mean of planetary-scale surface temperature computed by the Climatic Research Unit (Brohan et al. 2006) from 1850 to 2009. A nonlinear increasing trend is already visible concentrated in two periods, from 1910s to 1940s and then after 1975 (Fig. 2.3). Other datasets lead to the same conclusions (IPCC 2007).

Beyond GHG variations, there are two major "external" forcings operating at timescales between 1 and ~100 years: (i) the solar "constant" varies and we are now in cycle 24 of an 11-year cycle (the last minimum occurred in 2007–2009; cf. http://www.climate4you.com/Sun.htm#Recent solar irradiance); (ii) explosive volcanism able to disseminate large amounts of sulfur dioxide in the stratosphere cools down the earth's surface by as much as 0.3 °C for 2–3 years, such as after the eruption at Pinatubo in June, 1991. Both forcings are estimated to be minor relative to the GHG variations (Fig. 2.3). Internal climate system interactions also superimpose some variations at these timescales. For example, the warm phase of the El Niño Southern Oscillation (as in 1997–1998, Fig. 2.3) transfers a large amount of heat from the upper levels of the tropical Pacific to the large-scale atmosphere, and thus adds a transient (lasting a few years at maximum) warming signal of a few tenths of degrees Celsius in global surface temperature (Klein et al. 1999). All these factors are combined with GHG increase and drive the temperature variations. Looking at a perfect match between mean temperature variations, that integrate all these causes, with the time evolution of a single forcing is physically wrong, and the natural climate variability is able to generate nonlinear variations even from a monotonic forcing, as the GHG increase. In that respect, numerical simulation is a decisive tool inasmuch as it allows multiple scenarios where the relative impact of each possible forcing could be compared and scaled, beyond basic estimate of their radiative forcing as shown in Table 2.1.

The increase of mean surface temperature during the twentieth century is not disputable. Moreover, it is also corroborated by other planetary-scale climatic variations that could hardly be explained by any alternative plausible factors. Two of

There are typically 4–6 such Rossby waves around the globe between subtropical and subpolar latitudes, that are the main factor determining the spatial scale of monthly or seasonal temperature anomalies at the extratropical latitudes) to zonal/near-global (as El Niño Southern Oscillation phenomenon) or even planetary scales (e.g., variations of the solar constant or GHG concentrations, large volcanic eruptions, etc.). The anomalies of temperatures relative to the annual cycle at monthly and moreover annual timescales have thus a far larger spatial coherence and less amplitude than localized records. In that way, it is possible, and physically plausible, because of the link between temperature variations and the change in radiative balance, to compute the spatial mean of surface temperature at continental or even planetary scales.

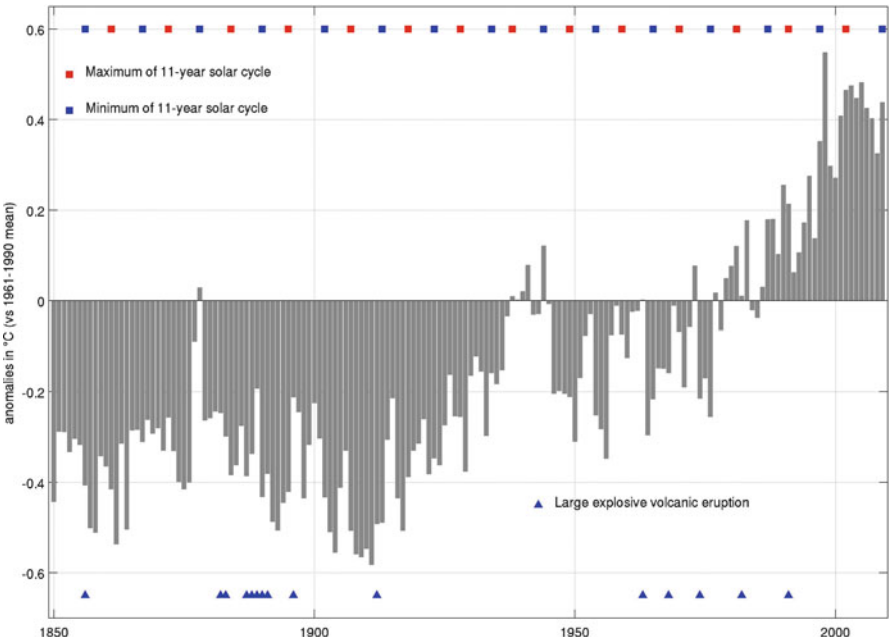

Fig. 2.3 Annual mean surface temperature from 1850 to 2009 expressed as anomalies in °C relatively to the 1961–1990 mean (from the Climatic Research Unit, Norwich, UK). Note that other estimates (such as the one provided by the Goddard Institute Space Studies, New York, USA) are very consistent. The *red* and *blue squares* on the *top* indicate, respectively, the maximum and minimum of the 11-year solar cycle (i.e., sunspot cycle). The solar constant variation is close to ~1 W/m^2 from minimum to maximum of the 11-year cycle, that is, equivalent to a radiative forcing of ~0.17 W/m^2. A slower variation is superimposed on the 11-year solar cycle, but its amplitude is still uncertain with a maximum of ~2 W/m^2 (equivalent to a radiative forcing of ~0.34 W/m^2) between a minimum in the late nineteenth century and a maximum in the second half of the twentieth century. The *blue triangles* at the *bottom* indicate a major volcanic eruption able to inject a massive amount of sulfur into the stratosphere. These volcanic eruptions could have a radiative forcing close to −0.5 to −3.3 W/m^2 in three years from the eruption at maximum. Note that such volcanic eruptions are absent from 1913 to 1962, then from 1992 onwards. For example, the eruption of Eyjallajökull in April 2010 was not explosive enough to inject sulfur into the stratosphere and its planetary-scale forcing is thus negligible

these interrelated variations are (i) sea level rise and (ii) the melting of most of mountain glaciers. The mean sea level rose by ~20 cm since 1870 (+1.7 mm/year during the twentieth century) and the rate of rises has recently increased (Church and White 2006). The recent rate of global mean sea level rise measured by satellite (since 1993) equals +3.3 mm/year with ~30 % due to thermal expansion and ~55 % from mass loss in mountain glaciers and ice sheets (Cazenave and Llovel 2010). Worldwide glaciers have been shrinking significantly with strong retreats in the 1940s, followed by stable or growing conditions around the 1970s and again increasing rates of ice loss from 1985 onward (UNEP 2008). The reaction of a single glacier is not only linked to local temperature variations but also changes in solar

radiation as well as cloudiness, amount and annual cycle of precipitation, and so on. But the fact that almost all mountain glaciers retreat at the same time should be considered as a fingerprint of current global warming.

2.5 Numerical Simulation of the Climate System

Global climate models (GCM) are mathematical artifacts of the climate system based on physical laws translated into mathematical equations. The climate system is discretized in 3D gridboxes. Some physical principles are explicitly described whereas some processes (such as convection) should be parameterized with ad hoc equations because of unresolved scales (Trenberth 1993). GCMs differ mostly by their horizontal and vertical resolutions, parameterizations, integration of different submodels (the current minimal set includes ocean, atmosphere, and a land–surface–vegetation scheme), and the way to compute numerical estimates on the grid. GCMs allow the running of numerical experiments with a single or a combination of plausible radiative forcings. It allows separating the cause of variations and the climate system response. This advantage is decisive when there are no known historic or paleoclimatic analogues (as in the case of the current GHG increase). GCMs are in fact not perfect and they remain considerably "simple" compared to the true climate. Nevertheless, the comparison between the first IPCC crude predictions of sea level rise and temperature increase made in 1990 and the observations until 2008 is very encouraging about the ability of current GCMs to simulate a realistic response to well-calibrated radiative forcing as the current GHG increase (Rahmstorf et al. 2007).

Basically, there are three types of uncertainty regarding the near-future numerical simulations of the climate: (i) the uncertainty linked to the simulation of the response to large and regional-scale forcing; (ii) the uncertainty linked to the amount of the future GHG emissions; and (iii) the uncertainty linked to the relative and/or absolute impact of other forcings. These uncertainties are considered in different ways.

The first uncertainty is inherent to any modeling because (i) the climate system integrates a continuum of time and spatial scales that could not be explicitly and fully considered (i.e., we cannot explicitly simulate all air molecules and our knowledge of the whole climate system is far from comprehensive) and (ii) the climate system is chaotic, that is, very sensitive to initial conditions. This means that a single numerical experiment contains one part related to the forcing (i.e., "forced" response) but also another part coming from the initial conditions and which is "free," that is, not reproducible (i.e., another experiment with exactly the same forcing but different initial condition leads to a different output). We need to have a probabilistic approach by running multiple experiments with the same or, better, different GCMs to estimate the intensity and shape of the forced response relative to the free one. The fact that the climate system is chaotic does not forbid probabilistic long-term prediction as soon as the forced response surpasses the free one for a given time and spatial scale. For example, the exact temperature on July 14th or January 1st, 2100 in Paris will be unknown until 10–15 days before, but we can predict that July 2100 will be warmer

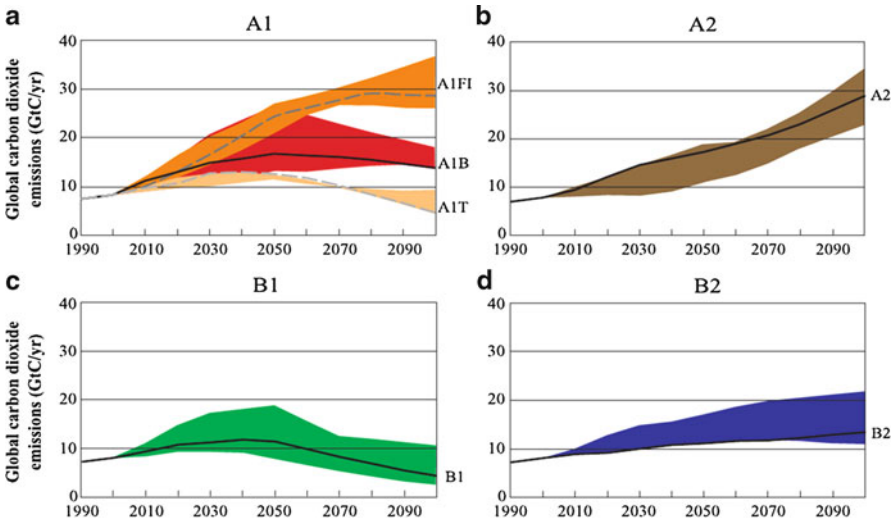

Fig. 2.4 Total global annual CO_2 emissions from all sources from 1990 to 2100 in gigatonnes of carbon per year (GtC/year) for the six scenario groups (panel **a**: A1Fl in orange, A1B in red and A1T in light orange; panel **b**: A2 in brown; panel **c**: B1 in green; panel **d**: B2 in blue). The 40 SRES scenarios are presented by the 5 scenario groups with each colored emission band showing the scenario range within each group. The equivalent radiative forcing (in 2100 relatively to 1990) ranges from around +3 W/m^2 (B1) to +7 W/m^2 (A1FI and A2) (IPCC 2007) (*Climate Change 2007: Synthesis Report.* Contribution of Working Groups I, II and III to the Fourth Assessment Report of the Intergovernmental Panel on Climate Change, Figure 3.2. IPCC, Geneva, Switzerland)

in mean than January 2100 in Paris because (i) a month is considered instead of a single day, (ii) the thermal difference between January and July 2100 in Paris (and all northern extratropical and subtropical zones) is primarily forced by the annual cycle of solar radiation between these 2 months, and (iii) the prediction of the polarity and the amplitude of this forcing is almost certain. On the contrary, this does not say anything about the temperature variation between January 1st, 2100 and the next day because this variation relies partly on the precise atmospheric state, which is unpredictable before December 15th to 20th, 2099 at best. Prediction of the climate response to atmospheric GHG increase is a climatic prediction of the same type as the temperature response to the annual cycle of the solar radiation.

The second uncertainty is explicitly taken into account through a whole range of scenarios considering mostly demographic growth, socioeconomic variations and technological efforts. The first scenarios, called IS92, were defined in 1992. The scenarios developed in 1996 for the IPCC third assessment report are broader. They include improved emissions baselines and allow the examination of different rates and trends of socioeconomic and demographic changes throughout the world. They are detailed in a special report of the IPCC.[11] There are a total of 40 scenarios and 6 scenario groups within 4 families (A1, A2, B1, and B2; Fig. 2.4) summarized here: A1FI

[11] See http://www.ipcc.ch/pdf/special-reports/spm/sres-en.pdf

(Fossil fuel Intensive), A1B (Balanced), and A1T (predominantly nonfossil fuel) are embedded in the A1 storyline, that is, a future world of very rapid economic growth, global population that peaks in the mid-twenty-first century and declines thereafter, and the rapid introduction of new and more efficient technologies. There is an expectation of global convergence among the countries. The three scenarios differ by their technological emphasis and the proportion of use of fossil fuel. The A2 storyline combines a continuously increasing global population and a less converging world (i.e., the economic growth is more regionally oriented) than in the A1 family. The B1 storyline describes the same population scenario as A1, but with a rapid transition of the economy toward service and information, including the introduction of clean and resource-efficient technologies. The B2 storyline describes a world with a moderate increase of global population coupled with emphasis on local solutions to economic, social, and environmental sustainability at local and regional levels. These scenarios include GHG but also sulfur emissions and are translated into equivalent total global annual CO_2 emissions from all sources (Fig. 2.4). The colored band shows the range of all scenarios for each group. The only group leading to a net reduction of global CO_2 emissions in 2100 relative to 1990 (~7 GtC/year) is the B1 and A1T group although the increase is moderate in B2 and A1B (roughly 13–15 GtC/year in 2100) and strong for A1FI and A2 (close to 30 GtC/year in 2100). The equivalent radiative forcing ranges from +2 W/m^2 (B1) to +7 W/m^2 (A1FI). Within each group, the scenario explores the differences and uncertainties in the driving forces. These emissions are then converted into GHG atmospheric concentrations. In summary, the 40 scenarios describe different pathways and cover a wide range of possible "futures." Note that the last estimate of the current growth rate of fossil-fuel emission (+3.5 %/year between 2000 and 2007) is above the largest predicted growth rate, that is, +2.7 %/year (AIFI) on 2000–2010.

The last uncertainty is related to the relative impact of GHG increase with other independent forcings operating at similar time scales (i.e., between 10 and 1,000 years). Many studies analyze the possible external forcings of the radiative balance of the earth. If we exclude major changes related to massive meteorites and/or comets falling on earth as the major impact occurring at Chixulub (Yucatan, Mexico) 65×10^6 years ago, there are two other possible forcing on the 10–1,000 years scale. The first one is the solar "constant" which exhibits an almost continuous scale of variation from seconds to billions of years. The 11-year cycle has a net radiative impact of 0.17 W/m^2 although longer (and less regular) 80–200 year cycles could have a net radiative impact of 0.3–0.7 W/m^2. The second natural forcing is related to major volcanic eruptions that could decrease the net radiation by 0.5–3.5 W/m^2 for 2–3 years. We do not know about the future evolution of the solar constant and even more, volcanic activity. But, we can hypothesize at least that variations of the solar constant similar to those experienced during the twentieth century are unable to add a significant signal to the GHG increase postulated by IPCC scenarios. In the same way, if volcanic eruptions keep the same variation as in the twentieth century (few significant eruptions before 1912, then after 1963 with the last one in 1991), its impact would be negligible.

2.6 Climate Projections for the Near Future

Figure 2.5 shows the evolution of mean annual temperatures for a set of scenarios. Each curve is the mean of multiple experiments (23 GCMs) and obviously filters the interannual–decadal variability. Even if the forcing is monotonic, the climatic response should be irregular with near-stationary periods interrupted by more or less abrupt increases. The superposition of additional factors reviewed just above will also add a degree of complexity to the planetary signal. Anyway, the global mean temperature in 2100 is expected to increase from +1.8 °C (B1) to +4 °C (A1FI) with the full range between +1.1 °C and +6.4 °C.[12] This signal is weak at the beginning of the twenty-first century and progressively increases in power as time goes by.

Even if the GHG increase is spatially uniform, the thermal response is heterogeneous with a larger increase over the continents, especially over the subpolar continents of the northern hemisphere, rather than over oceans (especially in the northern

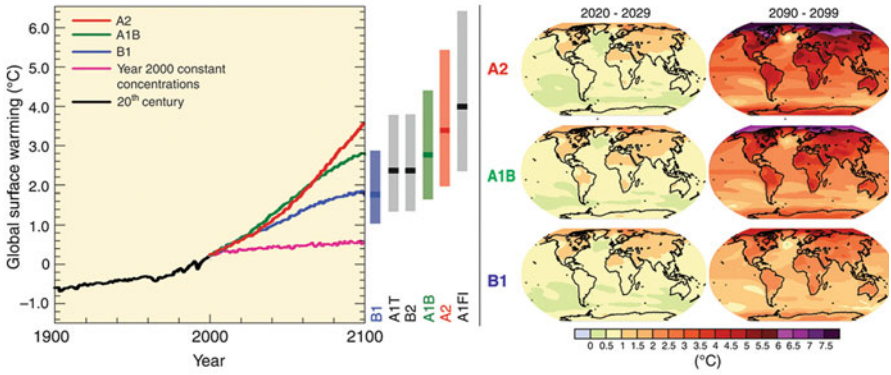

Fig. 2.5 *Left panel*: *Solid lines* are multimodel (23 models) global averages of surface warming for scenarios A2, A1B, and B1, shown as continuations of the twentieth-century simulations. These projections also take into account emissions of short-lived GHGs and aerosols. The *pink line* is not a scenario, but is for Atmosphere–Ocean General Circulation Model (AOGCM) simulations where atmospheric concentrations are held constant at year 2000 values. The *bars* at the *right* of the figure indicate the best estimate (*solid line within each bar*) and the likely range assessed for the six SRES marker scenarios at 2090–2099. All temperatures are anomalies in °C relative to the period 1980–1999. *Right panel*: Projected surface temperature change for the early (2020–2029) and late twenty-first century (2080–2099). The map shows the multi-AOCGM average projection for the A2, A1B, and B1 SRES scenario. Temperatures are anomalies in °C relative to the period 1980–1999 (IPCC 2007) (*IPCC 2000: Special Report on Emissions Scenarios*. Prepared by Working Group III of the Intergovernmental Panel on Climate Change, Figure SPM-3. Cambridge University Press)

[12]Note that the thermal difference between glacial and interglacial periods during the quaternary equals 6–10 °C in Antarctica and Greenland.

Atlantic and around Antarctica; Fig. 2.5). This emphasizes the role of positive and negative feedback that, respectively, amplify and weaken the temperature increase. For example, the response is weaker across the ocean partly because of the thermal vertical structure of the ocean with an efficient vertical mixing of the heat and also the infinite source of water, thus limiting the surface temperature increase through evaporation. On the contrary, the response will be stronger for the continents having a current seasonal snow cover and where its duration will decrease as the temperature increases (Fig. 2.5). In that case, the replacement of the snow cover/sea ice by open water, vegetation, or soils during a certain amount of time will greatly increase the amount of absorbed solar radiation (because snow reflects 80–95 % of incident solar radiation whereas water or vegetation absorbs 85–99 % of incident solar radiation) and thus amplify the response. The amplification could also be due to the vertical structure of the atmosphere (i.e., vertical thermal inversion in the lower troposphere as above subpolar continents in winter and permanent icy surfaces). The response will also be stronger over the continents where soils become drier in consequence of higher temperature, especially in spring and summer (Fig. 2.5). In that case, latent heat will decrease and sensible heat and IR emission will increase, thus amplifying the temperature increase. These examples above illustrate the negative and positive feedback that modulate the local-scale response to a planetary-scale forcing as the GHGs increase. Note that all climatic variables more or less controlled by temperature, such as sea level, will follow it with a similar degree of certainty. The uncertainty is far larger for climatic variables mostly controlled by atmospheric circulation, especially extreme events (extratropical storms or tropical cyclones). For example, the net effect of GHG atmospheric concentration increase is unclear on annual precipitation even if some tendency begins to emerge such as more precipitation in subpolar latitudes and less rainfall for subtropics (including the Mediterranean basin, e.g.) (IPCC 2007).

2.7 Conclusion

The climate system is a thermodynamical engine fueled by solar radiation. The radiative equilibrium between the absorbed incoming solar radiation and outgoing emitted earth radiation determines its mean temperature. Some atmospheric traces (gaseous H_2O, CO_2, CH_4, N_2O, etc.) accounting for less than 1 % of air absorbs a lot of infrared radiation although they are almost transparent to visible light, thus increasing the amount of absorbed energy by the atmosphere and earth surface. The GHG atmospheric concentration increases due to various human activities increases monotonically, with an increased rate from the 1950s and thus forces a warming of the global surface temperature. In fact, the global surface temperature has increased mostly from 1910 to 1940 and from 1975. This increase is fully consistent with global-scale variations as sea-level rise and the melting of most of the mountain glaciers during the twentieth century. Even if the global surface temperature variations are not only controlled by GHG atmospheric concentration, there is a large

consensus about the significant role of its current increase, especially during the second half of the twentieth century.

For the next centuries, if large explosive volcanic eruptions injecting a large amount of sulfur above 12–18 km do not occur every 2–3 years, if solar constant variations are similar to those experienced in the last centuries at least, and lastly if we exclude extremely rare events as the collision with a massive meteorite, then the main forcing to temperature variations will be the GHG atmospheric concentration increase due to human activities.[13] Despite the Kyoto Protocol[14] ratified in 1997 and ending in 2012 (currently extended till 2020), the current increase of fossil-fuel emission from 2000 is slightly above the "worst" IPCC scenario (i.e., A1FI). Global warming is thus virtually certain, in response to the increase of heat trapped by the climatic system and the continuous restoration of the radiative balance, but its rate and amplitude depend either on human choices or natural processes such as the oceanic ability to remove some of excess carbon from the atmosphere.[15] The whole scope of the IPCC scenario helps us to consider a wide range of possible future pathways. In that context, the increase of global surface temperature is also virtually certain during the twenty-first century (and beyond) and should be between +1.8 °C and +4 °C in 2100 (+6.4 °C if we follow the A1FI scenario until 2100). Beyond the fact that human choices could slow and delay this increase, it will be modulated in space and in time, even if other forcings are kept constant, due to the intrinsic nature of the climate system and the interplay of physical processes able to amplify/weaken the response at regional and zonal scales. The consequences of GHG increase on variables more or less controlled by temperature are also virtually certain such as the sea-level rise or the decrease of extent and/or of duration of snow cover or sea ice. The consequences are less clear for the hydrological cycle but higher temperatures will increase potential evaporation and will dry soils even if rainfalls are constant.

Acknowledgments I thank B. Hamelin and J. Guiot (CEREGE) for their careful reading.

References

Arrhenius SA (1896) On the influence of carbonic acid in the air upon the temperature of the ground. Philos Mag J Sci Ser 5, 41:237–276

Broecker WS (1975) Climatic change: are we on the brink of a pronounced global warming. Science 189:460–463

[13] This hypothesis also excludes engineering solutions able either to remove massive amounts of carbon from the atmosphere or to increase the earth's albedo.

[14] See http://unfccc.int/kyoto_protocol/items/2830.php.

[15] This ability should decrease with time—and perhaps saturate—inasmuch as the ocean acidifies itself as it absorbs more and more carbon. The recent estimates show that sinks of Carbon averaged since 1959 equal respectively: atmosphere (44 % of total Carbon anthropogenic emissions), land (28 %), ocean (28 %) (Le Quéré et al. 2012).

Brohan JJ, Kennedy I, Harris SFB, Tett S, Jones PD (2006) Uncertainty estimates in regional and global observed temperature changes: a new dataset from 1850. J Geophys Res 111:D12106. doi:10.1029/2005JD006548

Cazenave A, Llovel W (2010) Contemporary sea level rise. Annu Rev Mar Sci 2:145–173

Church JA, White NJ (2006) A 20th century acceleration in global sea-level rise. Geophys Res Lett 33:L01602. doi:10.1029/2005GL024826

Danny Harvey LD (2000) Global warming, the hard science. Prentice Hall, New York, 336 pp

Fourier J (1827) Mémoires sur les températures du globe terrestre et des espaces planétaires (Memoir on the temperature of the earth and planetary spaces). Mémoires de l'Académie Royale des Sciences de l'Institut de France, tome VII: 570–604

IPCC (2007) Synthesis report. IPCC, Geneva, 52 pp. Available at: http://www.ipcc.ch/publications_and_data/publications_ipcc_fourth_assessment_report_synthesis_report.htm

Klein SA, Soden BJ, Lau NC (1999) Remote sea surface temperature variations during ENSO: evidence of a tropical atmospheric bridge. J Climate 12:917–932

Le Quéré C, Andres RJ, Boden T, Conway T, Houghton RA, House JL, Marland G, Peters GR, van der Werf G, Ahlström A, Andrew RM, Bopp L, Canadell JG, Ciais P, Doney SG, Enright C, Friedlingstein P, Huntingford C, Jain AK, Jourdain C, Kato E, Keeling RF, Klein GK, Levis S, Levy P, Lomas M, Poulter B, Raupach MR, Schwinger J, Stich S, Stocker BD, Viovy N, Zaehle S, Zeng N (2012) The global carbon budget 1959–2011. Earth Syst Sci Data Dis 5:1107–1157. doi:10.5194/essdd-5-1107-2012

Lorius C, Jouzel J, Raynaud D, Hansen JA, Le Treut H (1990) The ice core: climate sensivity and future greenhouse warming. Science 347:139–145

Plaut G, Vautard R, Ghil M (1995) Interannual and interdecadal variability in 335 years of Central England temperatures. Science 268:710–713

Rahmstorf S, Cazenave A, Church JA, Hansen JA, Keeling RF, Parker DE, Somerville RCJ (2007) Recent climate observations compared to projections. Science 316:709

Schmidt GA, Ruedy RA, Miller RL, Lacis AL (2010) Attribution of the present-day greenhouse effect. J Geophys Res 115:D20106. doi:10.1029/2010JD014287

Shakun JD, Clark PU, He F, Marcott SA, Mix AC, Liu Z, Otto-Bliesner B, Schmitter A, Bard E (2012) Global warming preceded by increasing carbon dioxide concentrations during the last deglaciation. Nature 484:49–54. doi:10.1038/nature10915

Trenberth KE (ed) (1993) Climate system modeling. Cambridge University Press, New York, Xxix + 788 pp

Trenberth KE, Fasullo JK, Kiehl JT (2009) Earth's global energy budget. Bull Am Soc 90:311–323

UNEP (2008) Global glaciers changes: fact and figures. World Glacier Monitoring Service, Zurich, 88 pp. Availabe at: www.grid.unep.ch/glaciers